Research Square

Preprints are preliminary reports that have not undergone peer review.
They should not be considered conclusive, used to inform clinical practice,
or referenced by the media as validated information.

CircCAMSAP1 promotes osimertinib resistance in NSCLC by stabilizing HSPA1A through inhibition of SMURF1-mediated ubiquitination

Wenmei Su

suwenmei123@hotmail.com

Affiliated Hospital of Guangdong Medical University

Miao Yin

Yongyang Chen

Jinhui Chen

Xiaoqing Xu

Xiaobi Huang

Affiliated Hospital of Guangdong Medical University

Xiao Lei

Yanfeng Liang

Yuetong Jiang

Jialin Chen

Yuexin Zheng

Yudong Guo

Quan Yang

Haiwen Li

Qihe Long

Article

Keywords:

Posted Date: September 18th, 2025

DOI: https://doi.org/10.21203/rs.3.rs-7552127/v1

License: This work is licensed under a Creative Commons Attribution 4.0 International License.
Read Full License

Additional Declarations: There is **NO** conflict of interest to disclose.

Abstract

Osimertinib resistance is a key obstacle to the long-term efficacy of epidermal growth factor receptor (EGFR)-targeted therapy in non-small cell lung cancer (NSCLC). This study identified circCAMSAP1 (hsa_circ_0001900), a circular RNA (circRNA), as a key driver of acquired resistance. Functionally, circCAMSAP1 promotes proliferation, migration, invasion, and drug resistance in vitro and tumor growth in vivo. CircCAMSAP1 is upregulated in drug-resistant NSCLC cells and promotes cell survival by enhancing autophagic flux. Mechanistically, circCAMSAP1 prevents ubiquitination and proteasomal degradation of HSPA1A by disrupting the interaction between heat shock protein family A (Hsp70) member 1A (HSPA1A) and Smad-specific E3 ubiquitin protein ligase 1 (SMURF1). HSPA1A, a member of the HSP70 family, restores osimertinib sensitivity by targeting HSPA1A in vitro and in vivo by its allosteric inhibitor, JG-231. In addition, we found that the RNA-binding protein HnRNPA1 promotes the biogenesis of circCAMSAP1 by recognizing intron flanking motifs. Our study reveals a previously unrecognized mechanism of drug resistance involving circRNA-mediated regulation of protein homeostasis targeting the HnRNPA1/circCAMSAP1/SMURF1/HSPA1A axis, elucidating the mechanism of action of circCAMSAP1 in NSCLC tumorigenesis and EGFR-TKI resistance, providing a new target for NSCLC resistance therapy.

INTRODUCTION

Non-small cell lung cancer (NSCLC) accounts for approximately 85% of all lung cancer cases and remains the leading cause of cancer-related deaths worldwide[1]. Activating mutations in the epidermal growth factor receptor (EGFR) gene define a molecular subtype of NSCLC that is initially sensitive to EGFR tyrosine kinase inhibitors (TKIs). The third-generation EGFR-TKI, osimertinib, has become the standard of care for patients with sensitizing EGFR mutations or T790M resistance mutations due to its superior efficacy and central nervous system penetration[2]. However, despite initial clinical benefits, the inevitable development of acquired resistance severely limits the long-term effectiveness of osimertinib therapy[3].

Multiple mechanisms of osimertinib resistance have been identified, including secondary EGFR mutations, bypass signaling activation, phenotypic transformation, and changes in drug metabolism[4]. However, in a substantial proportion of cases, the underlying causes of resistance remain undefined, suggesting the existence of non-genetic, epigenetic, or post-transcriptional mechanisms that facilitate tumor adaptation under drug pressure. Recent studies have pointed to circular RNAs (circRNAs)—a class of covalently closed non-coding RNAs—as emerging regulators in cancer biology[5]. Due to their high stability and tissue specificity, circRNAs have been implicated in various oncogenic processes[6], such as proliferation, metastasis, immune evasion, and therapy resistance[7–9]. However, their role in mediating resistance to third-generation EGFR-TKIs remains largely unexplored.

In addition to post-transcriptional functions, the upstream biogenesis of circRNAs is increasingly recognized to be tightly regulated by RNA-binding proteins (RBPs) and alternative splicing factors[10]. Several splicing factors—including Quaking (QKI), HNRNPA1, and RBM20—have been shown to bind intronic complementary sequences and promote back-splicing through intron pairing or exon skipping mechanisms[11, 12]. For instance, QKI enhances circRNA formation by bridging flanking introns, and its knockout suppresses linear transcript production while altering > 17% of cardiac circRNAs[13]. Likewise, splicing factors such as ESRP1 facilitate specific circRNA isoform production through regulation of alternative exon inclusion[10]. The involvement of EMT-related splicing regulators suggests a mechanistic link between splicing plasticity and circRNA-mediated tumor adaptation under stress conditions[14, 15]. Beyond their role as miRNA sponges, circRNAs have also been shown to regulate protein ubiquitination and autophagic flux through direct interaction with key regulatory proteins. For example, circFOXO3 forms a ternary complex with MDM2 and p53 to promote MDM2-mediated ubiquitination and degradation of p53, thereby influencing cell cycle and apoptosis pathways[16]. Similarly, circEIF4G3 plays a tumor inhibitory role in gastric cancer by promoting TRIM25-mediated ubiquitination of δ-catenin degradation[17]. On the autophagy front, circRNAs such as circHIPK3 accelerate autophagy by modulating ATG gene expression through miRNA sponging[18], and circCDYL has been reported to enhance autophagic flux via the miR-1275-ATG7/ULK1 axis in breast cancer cells[19]. Since both ubiquitin-mediated degradation and enhanced autophagy are established resilience mechanisms under drug-induced stress, circRNAs capable of modulating these pathways emerge as plausible non-genetic drivers of therapeutic resistance.

However, their role in mediating resistance to third-generation EGFR-TKIs remains largely unexplored. Whether circRNAs directly influence osimertinib resistance by regulating ubiquitin-mediated degradation or autophagic response remains unknown, representing a critical gap in our understanding of post-transcriptional mechanisms of drug adaptation. In this study, we sought to systematically investigate the circRNA landscape associated with osimertinib resistance in NSCLC. Through transcriptome-wide circRNA profiling of resistant and parental NSCLC cell lines, we identified circCAMSAP1 as an upregulated candidate in resistant cells. Functional assays demonstrated that circCAMSAP1 promotes resistance by enhancing cell survival and autophagy. Mechanistically, we discovered that circCAMSAP1 directly binds to the heat shock proteins HSPA1A, preventing its degradation by the E3 ubiquitin ligase SMURF1 and thereby stabilizing its expression. Furthermore, we identified the splicing factor HnRNPA1 as a key driver of circCAMSAP1 biogenesis through binding to flanking intronic sequences.

In this study,Our findings reveal a previously unrecognized HnRNPA1/CircCAMSAP1/SMURF1/HSPA1Asignaling axis that facilitates osimertinib resistance through regulation of protein stability and autophagic activity. These insights not only expand our understanding of circRNA function beyond canonical ceRNA mechanisms but also identify potential therapeutic targets to overcome EGFR-TKI resistance in NSCLC.

RESULTS

CircCAMSAP1 is identified as a highly upregulated circular RNA in osimertinib-resistant NSCLC cells

Increasing evidence has indicated the involvement of circRNAs in various cancer-related processes. To investigate circRNAs that may mediate osimertinib resistance in NSCLC, we first progressively stimulated parental cell lines (PC9 and H1975) with long-term low-concentration osimertinib until stable osimertinib-resistant NSCLC cell lines (PC9/OR and H1975/OR) were screened. We then measured the cell IC50 values by the WST-1 assay, confirming the resistance of these two cell lines to osimertinib (Fig. 1A). Our results show that two osimertinib-resistant cell lines are not sensitive to osimertinib compared to parental cell lines and exhibit faster growth rates under osimertinib treatment (Supplementary Figures S1A-B). Next, we performed circRNA next-generation sequencing on PC9 and PC9/OR cells, as they showed the most significant differences between parental and drug-resistant cells, and identified 8 significantly upregulated circRNAs in PC9/OR cells (fold change of > 2 and p-value of < 0.05) compared to parental cells (Fig. 1B). We focused on circCAMSAP1 (hsa_circ_0001900)due to its potential functional relevance in drug resistance. As a circRNA derived from the CAMSAP1 gene family, which is involved in cytoskeletal organization and cellular stability, circCAMSAP1 may contribute to mechanisms underlying cancer cell adaptation. However, its role in NSCLC remains unexplored, highlighting the need for further investigation. To further confirm the circular nature and biogenesis of circCAMSAP1, we analyzed its genomic origin and circular junction. CircCAMSAP1 is derived from exon 2 and exon 3 of the CAMSAP1 gene located on chromosome 9. Sanger sequencing validated the head-to-tail splicing junction generated by back-splicing, consistent with the formation of a circular RNA (Fig. 1C).To distinguish circCAMSAP1 from its linear transcript, we performed RNase R digestion assays in PC9/OR and H1975/OR cells. RNase R selectively digests linear RNAs, while circular RNAs are resistant due to their closed-loop structure. As expected, CAMSAP1 mRNA levels were markedly reduced following RNase R treatment, whereas circCAMSAP1 levels remained stable, indicating strong resistance to exonuclease degradation (Fig. 1D). These findings confirmed that circCAMSAP1 exists in a circular configuration. To validate this further, we conducted PCR using divergent primers specific to circCAMSAP1 and convergent primers for linear CAMSAP1 and GAPDH on both complementary DNA (cDNA) and genomic DNA (gDNA) templates. The divergent primers amplified circCAMSAP1 only in cDNA, but not in gDNA, while linear CAMSAP1 and GAPDH were detected in both templates (Fig. 1E). These results further support the back-splicing origin of circCAMSAP1 and exclude the possibility of genomic DNA contamination or rearrangement.To explore the potential mechanism of action of circCAMSAP1, we examined its subcellular localization. Nuclear and cytoplasmic RNA fractions were isolated from PC9/OR and H1975/OR cells. Quantitative RT-qPCR analysis revealed that circCAMSAP1 was predominantly localized in the cytoplasm, whereas U6 mRNA and GAPDH mRNA were mainly distributed in the nucleus and cytoplasm, respectively (Fig. 1F). The cytoplasmic enrichment of circCAMSAP1 suggests it may function through post-transcriptional mechanisms, potentially by acting as a microRNA sponge or interacting with RNA-binding proteins.

CircCAMSAP1 promotes proliferation, migration, invasion, and osimertinib resistance in NSCLC cells

In order to investigate the potential role of circCAMSAP1 in mediating osimertinib resistance, we first examined its expression levels in both parental and resistant NSCLC cell lines. Quantitative RT-qPCR analysis revealed that circCAMSAP1 was significantly upregulated in both PC9/OR and H1975/OR cells compared to their respective parental lines (Fig. 2A), suggesting an association with acquired resistance.To explore its functional relevance, we designed two independent siRNAs (sicircCAMSAP1-1 and sicircCAMSAP1-2) targeting the back-splice junction of circCAMSAP1 and efficiently knocked down circCAMSAP1 expression in PC9/OR and H1975/OR cells without affecting the linear CAMSAP1 transcript (Fig. 2b). We further evaluated the impact of circCAMSAP1 knockdown on the long-term proliferative capacity of resistant cells using colony formation assays. CircCAMSAP1 knockdown significantly impaired the cloning ability of PC9/OR and H1975/OR cells (Fig. 2C). Next, we assessed the effect of circCAMSAP1 knockdown on cell viability. WST-1 assays showed that circCAMSAP1 knockdown significantly suppressed the proliferation of both PC9/OR and H1975/OR cells over time (Fig. 2D). In addition, dose-response analysis showed that circCAMSAP1 depletion significantly increased the sensitivity of resistant cells to osimertinib, as evidenced by a decrease in IC_{50} values in both cell lines (Fig. 2E), suggesting that circCAMSAP1 contributes to drug resistance, which reinforces its role in promoting resistance-associated survival and growth. As drug-resistant cancer cells often exhibit enhanced migratory and invasive potential, we performed transwell migration and invasion assays. The results showed that circCAMSAP1 knockdown substantially reduced both migration and invasion in PC9/OR and H1975/OR cells (Fig. 2F), this suggests that circCAMSAP1 may facilitate metastatic traits in osimertinib-resistant NSCLC. In conclusion, these results indicate that circCAMSAP1 promotes proliferation, invasion, migration, and osimertinib resistance in NSCLC cells.

CircCAMSAP1 facilitates tumor growth and resistance to osimertinib in vivo

To verify the relevance of circCAMSAP1 in mediating osimertinib resistance in vivo, a mouse xenograft model was established using PC9/OR cells transfected with shCtrl or shcircCAMSAP1 lentivirus (see Fig. 3A for a visual representation of this process). After tumor cell implantation, mice were treated with intraperitoneal injections of DMSO or osimertinib (Osi) for three weeks. Tumor growth and treatment response were monitored in four experimental groups: shCtrl + DMSO, shCtrl + Osi, shcircCAMSAP1 + DMSO, and shcircCAMSAP1 + Osi. Tumor-bearing mice were sacrificed at the endpoint, and gross morphology and tumor size suggest that circCAMSAP1 knockdown significantly enhances osimertinib sensitivity. Mice in the shcircCAMSAP1 + Osi group exhibit significantly smaller tumors compared to the control group (see Fig. 3B-C). Tumor growth curves showed that depletion of circCAMSAP1 alone modestly inhibited tumor growth, while circCAMSAP1 knockdown in combination with osimertinib significantly inhibited tumor progression (Fig. 3D). Consistent with these observations, the final tumor volume and tumor weight were significantly reduced in the shcircCAMSAP1 + Osi group compared to other treatment groups (Fig. 3E-F), suggesting that circCAMSAP1 knockdown enhanced the anti-tumor efficacy of osimertinib in vivo. To further explore the molecular basis of this enhanced sensitivity, tumor sections were subjected to immunohistochemical staining (IHC). Ki-67 staining showed a significant decrease in proliferative activity in the shcircCAMSAP1 + Osi group, as well as a significant decrease in the expression of the downstream target protein HSPA1A in this group (Fig. 3G). These findings

prompted us to further investigate the downstream mechanisms of circCAMSAP1-mediated osimertinib resistance.

CircCAMSAP1 facilitates autophagic activity in resistant NSCLC cells

To further investigate the underlying mechanism by which circCAMSAP1 promotes osimertinib resistance, we tested whether circCAMSAP1 is involved in autophagy, a process known to affect drug sensitivity in cancer cells. Western blot analysis showed that silencing circCAMSAP1 in PC9/OR and H1975/OR cells resulted in a significant accumulation of p62 and a decrease in LC3B-II levels, suggesting impaired autophagy flow (Fig. 4A-B). These observations suggest that circCAMSAP1 has a positive regulatory effect on autophagy in drug-resistant NSCLC cells. To distinguish between the possibility that the reduction of LC3B-II is due to reduced autophagosome formation or an enhanced degradation process, we treated the cells in question with chloroquine (CQ), a drug that acts as an autophagy inhibitor and is able to block lysosomal degradation. In the presence of CQ, LC3B-II levels were restored after circCAMSAP1 knockdown, suggesting that the reduction in LC3B-II observed in the absence of CQ was due to autophagic flow retardation rather than decreased autophagosome synthesis (Fig. 4C-D). To further validate these observations, a tandem mRFP-GFP-LC3 reporter system was used in drug-resistant NSCLC cells to monitor autophagosome and autophagolysosome formation. In untreated cells, circCAMSAP1 knockdown resulted in only red (autophagolysosome) spots and a significant reduction in total LC3 spots, indicating inhibition of the autophagic process. After CQ treatment, the accumulation of yellow spots (GFP and RFP combined) was observed in all groups, but significantly less in cells in the circCAMSAP1 knockdown group, further confirming the reduction of autophagic flux (Fig. 4E and Supplementary Figure S2A). Similarly, transmission electron microscopy (TEM) results further showed that circCAMSAP1 knockdown reduced the number of autophagosomes in drug-resistant NSCLC cells compared to the control group, while the number of autophagosomes in all groups increased after CQ treatment, suggesting that chloroquine inhibited the degradation process of autophagosomes(Fig. 4F). The observed knockdown of circCAMSAP1 has been shown to hinder the autophagy process, which may therefore enhance the sensitivity of cells to the effects of the drug.

CircCAMSAP1 binds to HSPA1A and enhances its expression to sustain resistance and autophagy

To further elucidate the molecular mechanisms by which circCAMSAP1 functions, RNA pull-down experiments were performed using biotinylated circCAMSAP1-specific probes, followed by SDS-PAGE and mass spectrometry analysis (Fig. 5A). Among the enriched proteins, HSPA1A was identified as a major binding candidate (Fig. 5B-C), suggesting a potential interaction between circCAMSAP1 and HSPA1A. To verify this interaction, we performed RNA immunoprecipitation (RIP) experiments using anti-HSPA1A antibodies. Subsequent PCR and RT-qPCR analyses confirmed that circCAMSAP1 was significantly enriched in HSPA1A immunoprecipitates compared to the IgG control, while no linear CAMSAP1 mRNA was detected (Fig. 5D-E), confirming the specificity of the interaction. To further investigate the expression of HSPA1A in osimertinib-resistant NSCLC cells, Western blotting and RT-qPCR analysis showed that HSPA1A was significantly upregulated in PC9/OR and H1975/OR cells

compared to its parental cell line (Supplementary Figure S3A-B). Next, we examined the functional relevance of HSPA1A in circCAMSAP1-mediated drug resistance. First, we constructed a cell model of stable overexpression of HSPA1A using lentiviral vectors and detected it by western blotting and RT-qPCR analysis, and the expression level of overexpressed HSPA1A was significantly increased compared to the blank control group, indicating that the overexpression model was successfully constructed (Supplementary Figure S3C-D). Next, the WST-1 assay further revealed that overexpression of HSPA1A promoted osimertinib resistance in NSCLC cells (Supplementary Figure S3E-F). Colony formation experiments showed that overexpression of HSPA1A significantly increased the cloning ability of NSCLC cells (Supplementary Figure S3G-H). At the same time, overexpression of HSPA1A was observed by Western blotting to reduce the level of the autophagic substrate p62 protein and increase the level of the autophagosome formation marker LC3B protein, suggesting that it promotes autophagy (Supplementary Figure S3I-J). To further investigate the regulatory relationship between circCAMSAP1 and HSPA1A, colony formation experiments showed that clone formation of circCAMSAP1 alone inhibited clonal formation in PC9/OR and H1975/OR cells, and HSPA1A overexpression significantly restored this inhibition (Fig. 5F). Subsequent knockdown of circulation alone resulted CAMSAP1 reduced osimertinib IC50 in PC9/OR and H1975/OR cells, while overexpression of HSPA1A partially rescued the sensitive phenotype, manifested by an increase in IC50 values (Fig. 5G-H). These results suggest that HSPA1A acts downstream of circCAMSAP1, promoting osimertinib resistance. In addition, Western blotting showed that circCAMSAP1 knockdown inhibited HSPA1A protein levels, while p62 increased and LC3B-II decreased, suggesting inhibition of autophagy. Importantly, HSPA1A overexpression reverses these autophagy changes, further supporting its functional involvement (Fig. 5I-J). Taken together, these findings suggest that circCAMSAP1 partially promotes osimertinib resistance and autophagy in NSCLC cells by directly interacting with HSPA1A and regulating HSPA1A expression.

CircCAMSAP1 stabilizes HSPA1A protein by blocking SMURF1-mediated ubiquitination

To investigate how circCAMSAP1 regulates HSPA1A protein levels, we first examined the effect of circCAMSAP1 knockdown on HSPA1A expression. Western blotting showed that circCAMSAP1 knockdown significantly reduced HSPA1A protein levels (Fig. 6A), while RT-qPCR showed no significant change in HSPA1A mRNA levels (Supplementary Figure S4A). This also suggests that transcriptional levels may not be involved in the decrease in HSPA1A protein levels, suggesting that circCAMSAP1 may regulate HSPA1A stability through post-translational modifications (PTMs). To further validate our hypothesis and determine whether the reduction in HSPA1A is due to altered protein stability, we treated cells with cycloheximide (CHX) to inhibit protein synthesis and monitor HSPA1A degradation over time. The results showed that knockdown of circCAMSAP1 significantly reduced the half-life of HSPA1A protein, suggesting that circCAMSAP1 stabilized HSPA1A at post-translational levels (Fig. 6B). Next, we evaluated whether circCAMSAP1 knockdown affects HSPA1A degradation via the ubiquitin-proteasome pathway. Treatment with the proteasome inhibitor MG132 rescued HSPA1A protein levels after circCAMSAP1 knockdown (Fig. 6C), suggesting that circCAMSAP1 prevented proteasomal degradation of HSPA1A. We then performed co-immunoprecipitation of HSPA1A followed by ubiquitin immunoblotting, and circCAMSAP1 knockdown significantly enhanced the ubiquitination of HSPA1A

protein and its proteasome-mediated degradation compared to the negative control group (Fig. 6D), supporting the idea that circCAMSAP1 stabilizes HSPA1A expression by inhibiting its ubiquitination. Using the silico prediction tool Ubibroswer (http://ubibrowser.bio-it.cn/ubibrowser/home/index), we identified SMURF1, a known E3 ubiquitin ligase, as a potential regulator of HSPA1A (Supplementary Figure S4B). Western blotting showed that circCAMSAP1 knockdown resulted in an increase in SMURF1 protein levels (Supplementary Figure S4C), however, RT-qPCR showed no significant change in mRNA levels of SMURF1 (Supplementary Figure S4D). To validate the interaction of circCAMSAP1 with SMURF1, we performed RIP experiments with anti-SMURF1 antibodies, and subsequent RT-qPCR analysis showed that circCAMSAP1 was significantly enriched in SMURF1 immunoprecipitates compared to IgG controls (Fig. 6E). In addition, Western blotting showed that knockdown of SMURF1 resulted in a significant increase in HSPA1A protein levels and a decrease in SMURF1 own protein levels (Fig. 6F). RT-qPCR analysis showed that SMURF1 knockdown did not alter the mRNA levels of HSPA1A, while its own mRNA levels decreased (Supplementary Figure S4E-F), suggesting that SMURF1 mediates HSPA1A degradation downstream of circCAMSAP1. To further confirm this regulatory axis, we assessed the level of ubiquitination of HSPA1A in SMURF1-depleting cells. Co-immunoprecipitation results showed that SMURF1 significantly reduced the ubiquitination level of HSPA1A (Supplementary Figure S4G), supporting its role as an E3 ligase responsible for HSPA1A proteasome degradation. In addition, co-immunoprecipitation assays further confirmed the interaction between SMURF1 and HSPA1A (Fig. 6G). Next, co-immunofluorescence experiments were performed to evaluate the localization of HSPA1A and SMURF1, which showed that these two molecules were primarily colocalized in the cytoplasm of PC9/OR cells, and circCAMSAP1 knockdown promoted the colocalization of HSPA1A and SMURF1 (Supplementary Fig. 6H). Interestingly, co-immunocoprecipitation results showed that circCAMSAP1 knockdown enhanced the binding between SMURF1 and HSPA1A (Fig. 6H), suggesting that circCAMSAP1 may protect HSPA1A from degradation by interfering with SMURF1-HSPA1A interactions. Notably, circCAMSAP1 knockdown-mediated ubiquitination degradation of HSPA1A is dependent on SMURF1, as siSMURF1 was found to salvage circCAMSAP1-knockdown HSPA1A ubiquitination levels after co-transfection with sicircCAMSAP1 (Fig. 6I). Taken together, these findings reveal a novel regulatory mechanism: circCAMSAP1 enhances the stability of HSPA1A by preventing SMURF1-mediated ubiquitination and proteasomal degradation, thereby promoting osimertinib resistance in NSCLC cells.

The allosteric inhibitor JG231 reverses osimertinib resistance in lung adenocarcinoma in vitro and in vivo

To validate the functional importance of HSPA1A in mediating osimertinib resistance, we used the allosteric inhibitor JG-231 and evaluated its effects on drug-resistant NSCLC cells in vitro and in vivo. Treatment with JG-231 alone significantly inhibits the viability of PC9/OR and H1975/OR cells in a dose-dependent manner. Of particular note was the significant reduction in cell viability with the combination of osimertinib and JG-231 compared to osimertinib alone (Fig. 7A). The combination index (CI) values were calculated using compuSyn software to determine whether the combination produced synergistic cytotoxicity and CI values were found to be less than 1.0 in both PC9/OR and H1975/OR cell lines, indicating a synergistic antitumor effect (Fig. 7B). Next, we found that JG-231 treatment impaired the

colony-forming capacity of PC9/OR and H1975/OR cells in vitro, with the most pronounced inhibition at 4 μM concentrations (Fig. 7C). In addition, Western blotting showed that JG-231 potently inhibited HSPA1A expression in two drug-resistant cell lines, accompanied by an increase in p62 and a decrease in LC3B-II, suggesting that autophagy was inhibited in a dose-dependent manner, supporting its targeting activity (Fig. 7D). In vivo, the therapeutic potential of JG-231 was further evaluated using a PC9/OR-derived xenograft model. Treatment of mice with JG-231 in combination with osimertinib resulted in significantly slower tumor growth compared to monotherapy or control (Fig. 7E-F. The final tumor volume and tumor weight were significantly reduced in the combination group (Fig. 7G-H), and IHC of tumor tissue sections showed a significant reduction in the expression of the target protein HSPA1A in the JG-231 versus osimertinib group, confirming that inhibition of HSPA1A enhances anti-tumor efficacy in overcoming osimertinib resistance(Fig. 7I). These findings highlight HSPA1A as a key functional mediator of circCAMSAP1-induced resistance and demonstrate that JG-231 resensitizes drug-resistant NSCLC cells to osimertinib in vitro and in vivo by targeting HSPA1A.

HnRNPA1 promotes the biogenesis of circCAMSAP1

To investigate the upstream regulatory mechanisms of circCAMSAP1 upregulation in osimertinib-resistant NSCLC cells, we performed bioinformatics predictions (http://rbpmap.technion.ac.il/). Among the candidates, Western blotting and RT-qPCR showed that expression of HnRNPA1 was significantly upregulated in drug-resistant NSCLC cell lines compared to its parent cell lines (Fig. 8A). We further engineered two independent siRNAs targeting HnRNPA1 (siHnRNPA1-1 and siHnRNPA1-2), and Western blotting and RT-qPCR showed potent knockdown of HnRNPA1 expression in drug-resistant NSCLC cells (Supplementary Figure S5A-D). A series of experiments were performed to evaluate the role of HnRNPA1 in regulating circCAMSAP1 biosynthesis. Specifically, knockdown of HnRNPA1 resulted in a significant reduction in mRNA levels of circCAMSAP1, but did not affect the mRNA levels of linear CAMSAP1 transcripts, suggesting that HnRNPA1 regulates circCAMSAP1 expression (Fig. 8B). Splicing factors have been reported to drive circRNA cyclization by specifically recognizing and binding sequences in circRNA flanking introns[20]. In previous reports, HnRNPA1 can interact with these potential binding sites, TGGGGT and TAGAGA[21]. To determine the critical role of HnRNPA1-binding specific sequences of flanking introns in circCAMSAP1 circularization. Two potential HnRNPA1 binding sites were identified, one upstream of the circCAMSAP1 reverse splice site and the other downstream of the circCAMSAP1 site (Fig. 8C), and then wild-type and mutant circCAMSAP1 minigenes (minigenes) were designed for RIP experiments, and the results showed that HnRNPA1 specifically binds to wild-type binding sites for flanking introns, with no binding to the mutation sites observed (Fig. 8D). To functionally verify the importance of these binding sites, drug-resistant NSCLC cells were infected with or without minigene constructs (wild-type and various mutants) following HnRNPA1 knockdown, and RT-qPCR results showed that HnRNPA1 knockdown significantly reduced circCAMSAP1 production in transfected wild-type circCAMSAP1 mini-gene and single-site mutation (a-mut or b-mut) cells, however, in transfected two-site mutations (a/ b-mut), HnRNPA1 knockdown had minimal effect on circCAMSAP1 production, suggesting that both loci are required to promote efficient circCAMSAP1 biosynthesis (Fig. 8E). The

proposed working model is shown in Figure (Fig. 8F). In drug-resistant NSCLC cells, HnRNPA1 promotes circCAMSAP1 cyclization. circCAMSAP1 then promotes autophagy and cell survival by interacting with HSPA1A and stabilizing HSPA1A expression by inhibiting SMURF1-mediated HSPA1A ubiquitination and degradation. JG-231, an allosteric inhibitor targeting HSPA1A, has been shown to reverse this resistance phenotype, supporting the hypothesis that the circCAMSAP1-HSPA1A axis is a target for osimertinib resistance therapy in NSCLC.

DISCUSSION

The third-generation EGFR tyrosine kinase inhibitor (EGFR-TKI), osimertinib, has emerged as the standard first-line treatment for patients with NSCLC harboring activating EGFR mutations[22]. However, the clinical benefits of osimertinib are inevitably limited by the development of acquired resistance[23]]. Although multiple mechanisms of resistance have been described, including secondary EGFR mutations, activation of bypass signals, and histologic transformation[24, 25], these alterations account for only a subset of cases. This suggests that additional non-genetic mechanisms, particularly at the post-transcriptional and protein homeostatic levels, may play a key role in tumor adaptation[26]]. In recent years, circular RNAs (circRNAs), a class of stable and cell-type-specific noncoding RNAs, have emerged as important regulators in cancer biology[27, 28]. However, their potential role in osimertinib resistance remains largely unexplored.

In this study, we performed circRNA sequencing in osimertinib-sensitive and -resistant NSCLC cell lines and identified circCAMSAP1 (hsa_circ_0001900) as a significantly upregulated circRNA in resistant cells. Functionally, circCAMSAP1 promoted resistance by enhancing cell proliferation, migration, clonogenicity, and tumor growth in vitro and in vivo, while silencing circCAMSAP1 markedly restored sensitivity to osimertinib. Mechanistically, we demonstrated that circCAMSAP1 directly binds to HSPA1A, a key molecular chaperone, and prevents its interaction with the E3 ubiquitin ligase SMURF1, thereby inhibiting HSPA1A ubiquitination and stabilizing its protein expression. Stabilized HSPA1A, in turn, enhances autophagic flux and promotes cell survival under drug pressure. Furthermore, we identified HnRNPA1 as the splicing factor responsible for circCAMSAP1 biogenesis, as it binds to flanking intronic sequences and facilitates back-splicing. These findings collectively establish a novel HnRNPA1/circCAMSAP1/SMURF1/HSPA1Aaxis that links alternative splicing, circRNA function, protein stability, and autophagy-driven resistance.

Our findings offer mechanistic insights that extend beyond the conventional understanding of circRNA biology. While previous studies have predominantly focused on circRNAs acting as miRNA sponges or regulators of transcription[27, 29], our work demonstrates that circRNAs can function by modulating protein homeostasis through interference with ubiquitin-mediated degradation. This non-canonical mode of action significantly expands the functional repertoire of circRNAs[28] Moreover, although HSPA1A has been implicated in cellular stress responses and therapeutic resistance[30, 31], its post-translational regulation by circRNAs has not been previously described. The multilevel integration of splicing control,

noncoding RNA function, proteostasis modulation, and autophagy regulation revealed in this study underscores the complexity of non-genetic resistance mechanisms and highlights the importance of cross-talk between RNA and protein regulatory layers[32].

Despite the strength of our findings, several important limitations should be acknowledged. First, our study was primarily conducted in established NSCLC cell lines and mouse xenograft models. While these systems offer reproducible platforms for mechanistic interrogation, they may not fully recapitulate the complexity of the human tumor microenvironment, including stromal interactions, immune modulation, and spatial heterogeneity of resistance[33]. Thus, validation of the HnRNPA1/circCAMSAP1/HSPA1A axis in patient-derived organoids or clinical biopsy specimens will be essential to determine its clinical relevance and biomarker potential[33]. Second, our mechanistic focus on HSPA1A does not exclude the possibility that circCAMSAP1 may bind to other proteins or RNA species. Although RNA pull-down and RIP assays showed specificity for HSPA1A, mass spectrometry identified additional candidates that may contribute to the resistance phenotype through parallel or compensatory pathways[34]. A more comprehensive dissection of the circCAMSAP1-centered interactome is needed to uncover potential co-factors or context-specific regulators.

Third, although our data support that SMURF1 is the primary E3 ubiquitin ligase responsible for HSPA1A degradation, we cannot exclude the possibility that other E3 ligases or deubiquitinating enzymes (DUBs) may also participate in this process, particularly under therapeutic stress. The regulation of proteostasis —a dynamic balance between protein synthesis, folding, trafficking, and degradation—is governed by a highly interconnected network of over 600 E3 ligases and nearly 100 DUBs, many of which exhibit redundancy and stress-responsive regulation[35, 36]. In response to drug pressure, cells can rewire these networks to adapt to proteotoxic stress, potentially compensating for SMURF1 function or reversing HSPA1A ubiquitination through alternate enzymes[37]. Moreover, proteostasis is not limited to ubiquitin–proteasome machinery but also involves molecular chaperones (e.g., Hsp70) and selective autophagy pathways such as chaperone-assisted selective autophagy (CASA) and chaperone-mediated autophagy (CMA)[38]. Therefore, it is plausible that circCAMSAP1 modulates a broader protein quality control network, not solely by interacting with SMURF1, but potentially by influencing additional E3 ubiquitin ligases, deubiquitinases (DUBs), or chaperone–co-chaperone complexes. For example, CHIP/STUB1 functions as both an E3 ligase and Hsp70 co-chaperone, linking protein folding to degradation pathways via ubiquitination and even autophagy[39]. BAG family proteins, such as BAG-1 and BAG-3, assist in delivering chaperone-bound substrates to the proteasome or autophagosome, working in concert with CHIP[40, 41]. UCHL5, a common DUB present at the proteasome, can deubiquitinate substrates to fine-tune degradation signals[42]. Therefore, circCAMSAP1 may act directly – by scaffolding or sequestering these proteins; or indirectly – by altering partner or DUB activity. Future work should systematically assess whether circCAMSAP1 also coordinates components such as CHIP/STUB1, UCHL5, or BAG family cochaperones that may promote osimertinib resistance through parallel or synergistic mechanisms of protein homeostasis[43].

Fourth, although autophagy was clearly modulated in our model, the downstream consequences of circCAMSAP1-mediated autophagy enhancement remain partially defined. Whether this autophagy is primarily cytoprotective, pro-survival, or contributes to metabolic adaptation under TKI treatment warrants further exploration[44]. Additionally, the interaction between autophagy and apoptotic signaling in this context remains unclear. Autophagy and apoptosis are two fundamental but intricately connected stress-response pathways[45]. In many cancer types, autophagy acts as a survival mechanism under drug pressure by maintaining cellular energy homeostasis, mitigating oxidative stress, and delaying apoptotic onset[46]. However, depending on the cellular context, autophagy may also shift from a protective to a cytotoxic role, or even act as a prerequisite for apoptosis[47]. Crosstalk between these pathways is often mediated by shared molecular players such as Bcl-2 family proteins, p62/SQSTM1, Beclin-1, and ATG proteins, which can serve dual roles in promoting or inhibiting apoptotic progression depending on post-translational modifications and binding partners[48].

In our model, it remains unknown whether circCAMSAP1-induced autophagy enhances cell survival by preventing apoptosis, or alternatively primes cells for death by regulating pro-apoptotic signaling thresholds. Moreover, it is possible that circCAMSAP1 may regulate the expression or stability of key nodal regulators at the intersection of autophagy and apoptosis—such as Bcl-2, BAX, or caspase-8—through mechanisms beyond HSPA1A modulation. A more detailed temporal and functional dissection of circCAMSAP1-mediated autophagy–apoptosis dynamics will be necessary to understand whether autophagy serves as a resistance mechanism or a vulnerability that could be therapeutically exploited[49–51].

Finally, the therapeutic feasibility of targeting circCAMSAP1 or its RNA–protein interface remains to be tested in a preclinical pharmacological context. While our use of the HSPA1A inhibitor JG231 provides proof-of-concept that this pathway is druggable, specific RNA-based therapeutics—such as ASOs, CRISPR/Cas13-based tools, or RNA aptamers—need to be developed and optimized to target circCAMSAP1 selectively in vivo[52–54]. Future research may focus on several directions. First, determining whether circCAMSAP1 is detectable in patient blood or exosomes could inform its potential utility as a liquid biopsy biomarker for osimertinib resistance[55]. Second, targeting circCAMSAP1 or its interaction interface with HSPA1A using antisense oligonucleotides or small molecules could represent a novel therapeutic strategy. Third, systematic investigation of other circRNA–protein interactions involved in ubiquitination pathways could uncover broader regulatory paradigms in drug resistance.

CONCLUSION

In conclusion, our study identified circCAMSAP1 as a circular RNA that plays a key role in promoting osimertinib resistance in NSCLC. We demonstrate that circCAMSAP1 functions by binding to HSPA1A (Heat Shock Protein Family A (Hsp70) Member 1A) HSPA1A, thereby preventing its SMURF1-mediated ubiquitination and proteasome degradation. This stabilization enhances autophagic flux and promotes cancer cell survival under therapeutic pressure. Furthermore, we uncover HnRNPA1 as the upstream

splicing factor that drives CircCAMSAP1 biogenesis via intronic motif recognition, linking alternative splicing regulation to resistance mechanisms. Importantly, the allosteric inhibitor JG-231 targeting HSPA1A successfully reversed circCAMSAP1-induced resistance in vitro and in vivo, highlighting its potential as a therapeutic vulnerability.

Our findings establish a novel HnRNPA1/CircCAMSAP1/SMURF1/HSPA1A axis that integrates post-transcriptional and post-translational regulation in the context of drug resistance. These insights not only broaden our understanding of the functional repertoire of circRNAs beyond canonical miRNA sponging but also point to RNA–protein interactions as viable targets for overcoming EGFR-TKI resistance. Future studies investigating the clinical relevance of CircCAMSAP1 and its potential as a circulating biomarker may further pave the way for precision therapeutics in EGFR-mutant NSCLC.

MATERIALS AND METHODS

Cell lines and culture conditions

Human NSCLC cell lines PC9 and H1975 were obtained from [source or ATCC]. Cells were cultured in RPMI-1640 medium supplemented with 10% fetal bovine serum (FBS) and 1% penicillin–streptomycin at 37°C in a humidified incubator with 5% CO_2. To establish osimertinib-resistant cell lines (PC9/OR and H1975/OR), the parental cell lines (PC9 and H1975) were continuously exposed to progressively increasing concentrations of osimertinib-containing medium for a prolonged period until stable resistant cell lines (PC9/OR and H1975/OR) were selected, and osimertinib was used to maintain the drug resistance of the PC9/OR and H1975/OR cells, all of which were cultured in a humidified incubator at 37°C with 5% CO_2.

CircRNA sequencing and data analysis

Total RNA from PC9 and PC9/OR cells was extracted using TRIzol reagent (Invitrogen) and subjected to ribosomal RNA depletion. Libraries were constructed using a circRNA sequencing protocol and sequenced on the Illumina platform. Differentially expressed circRNAs were identified based on fold change > 2 and $p < 0.05$. Back-splice junctions were confirmed by Sanger sequencing.

RNase R treatment and RT-qPCR

Total RNA was treated with RNase R (3 U/μg, Epicentre) for 30 min at 37°C to enrich circular RNAs. Reverse transcription was performed using random hexamers and PrimeScript RT Kit (Takara). Quantitative PCR was performed using SYBR Green Master Mix (Thermo Fisher). GAPDH was used as internal control. Divergent primers were used to amplify circCAMSAP1, and convergent primers for linear CAMSAP1.

Nuclear and cytoplasmic RNA fractionation

Cytoplasmic and nuclear RNA fractions were isolated using the PARIS Kit (Invitrogen) according to the manufacturer's instructions. Enrichment of circCAMSAP1 was determined by RT-qPCR, with U6 and GAPDH serving as nuclear and cytoplasmic controls, respectively.

siRNA and plasmid transfection

Small interfering RNAs (siRNAs) targeting circCAMSAP1, SMURF1, and HnRNPA1 were synthesized by Suzhou Genepharma Co., Ltd. Transfections were performed using Lipofectamine RNAiMAX or Lipofectamine 3000 (Invitrogen). The full-length sequence of HSPA1A was inserted into the GV492 lentiviral vector for stable overexpression, which was supplied by Shanghai Genechem Co., Ltd. Cells were harvested 48–72 h post-transfection for analysis.

Cell viability and colony formation assays

Cell viability was assessed usingWST-1 Cell Proliferation and Cytotoxicity Assay Kit). Cells were seeded in 96-well plates and treated with osimertinib for 24–48 h. Absorbance was measured at 450 nm. For colony formation, 500 cells/well were seeded in 6-well plates, cultured for 10–14 days, fixed with 4% paraformaldehyde, and stained with crystal violet.

Migration and invasion assays

Cell migration and invasion assays were performed using Transwell chambers (8 μm pore size, Corning), with or without Matrigel coating. Cells (1×10^5) were seeded in serum-free medium in the upper chamber, and after 24–48 h, they were fixed with 4% paraformaldehyde, stained with crystal violet, and counted under the microscope.

mRFP-GFP-LC3 autophagy reporter assay

Cells were transfected with mRFP-GFP-LC3 plasmid and observed using confocal microscopy (Leica). Autophagic flux was evaluated based on the ratio of yellow (autophagosomes) to red (autolysosomes) puncta.

Western blotting and co-immunoprecipitation

Proteins were extracted using RIPA buffer with protease inhibitors. Antibodies against HSPA1A, LC3B, p62, SMURF1, GAPDH, and ubiquitin were used. For ubiquitination assays, cells were treated with MG132 (10 μM) for 6 h. Co-immunoprecipitation (co-IP) was performed using Protein A/G magnetic beads and target-specific antibodies.

RNA-pulldown assay and liquid chromatography-tandem mass spectrometry (LC–MS/MS)

The biotinylated circCAMSAP1 probe and RNA pulldown kit was provided by Guangzhou BerSinBio. The probe is conjugated to magnetic beads and incubated with a cellular protein extract according to the manufacturer's protocol, followed by protein molecule specific binding to the RNA probe. After adequate

elution, RNA probe-protein complexes are obtained. Finally, the protein type is identified using western blotting or mass spectrometry.

RNA immunoprecipitation (RIP)

The RIP kit is provided by Guangzhou BerSinBio. Immunoprecipitation was performed using anti-HSPA1A, anti-SMURF1, and anti-HnRNPA1 antibodies to obtain RNA-protein complexes and protein-bound RNA was purified according to the manufacturer's protocol. Finally, co-precipitated RNA is detected using PCR or RT-qPCR.

In vivo xenograft model

Four-week-old female BALB/c nude mice are injected subcutaneously with PC9/OR cells stably expressing sh-circCAMSAP1 or control vehicle. Mice were treated with DMSO or osimertinib (5 mg/kg/day) by intraperitoneal injection. Tumor volume is measured every 3 days and is calculated as: $V = (L \times W^2)/2$. Mice are sacrificed after 4 weeks; Tumors are excised for IHC and protein immunoassays. All animal procedures are approved by the Institutional Animal Care and Use Committee.

Immunohistochemistry (IHC)

The tumor tissue was fixed with 4% paraformaldehyde, embedded in paraffin, and subsequently tissue sectioned. and stained with antibodies against Ki-67 and HSPA1A. Then, we use a microscope to take pictures.

Statistical analysis

Data are presented as mean ± SD. Statistical comparisons were performed using two-tailed Student’s t-test or one-way ANOVA with Bonferroni correction. $P < 0.05$ was considered statistically significant. Graphs were generated using GraphPad Prism.

Declarations

COMPETING INTERESTS

The authors declare no conflicts of interest.

AUTHOR CONTRIBUTIONS

Conceptualization, W.S., M.Y., and Y.C., Methodology, Y.C., M.Y., J.C., X.X., X.H., X.L., Y.L., and Y.J., Formal Analysis, Y.Z., Y.G., Q.Y., H.L., and Q.L., Research Investigation, Y.C., J.C. (Jinhui), J.C. (Jialin), and X.X.;Writing—Manuscript Preparation, Y.M., Y.C., J.C. (Jinhui), and X.X., Writing—Reviewing and Editing,

W.S. and Y.Z., Visualization, X.X. and Y.J., Superintendent, W.S. and Q.L., Access to Funding, W.S. and Q.L. All authors have read and agree to the published version of the manuscript.

ACKNOWLEDGEMENTS

This work was supported by the National Natural Science Foundation of China (82073388); The Affiliated Hospital of Guangdong Medical University Clinical Research Program (LCYJ2020B005 and LCY2022DL002); the Natural Outstanding Youth Fund of Guangdong Province (2022B1515020090); Guangdong Provincial Key Laboratory of Autophagy and Major Chronic Non-communicable Diseases (2022B1212030003), Zhanjiang Key Laboratory of Tumor Microenvironment and Organoid Research, the high-level talents scientific research startup funds of the Affiliated Hospital of Guangdong Medical University (GCC2022012).

References

1. Y. Zhu, J. She, R. Sun, X. Yan, X. Huang, P. Wang, et al. Impact of Bone Metastasis on Prognosis in Non-Small Cell Lung Cancer Patients Treated with Immune Checkpoint Inhibitors: A Systematic Review and Meta-Analysis[J]. Front Immunol. 2024, 15: 1493773
2. S.G. Wu, J.Y. Shih. Management of Acquired Resistance to Egfr Tki-Targeted Therapy in Advanced Non-Small Cell Lung Cancer[J]. Mol Cancer. 2018, 17 (1): 38
3. J.B. Blaquier, S. Ortiz-Cuaran, B. Ricciuti, L. Mezquita, A.F. Cardona, G. Recondo. Tackling Osimertinib Resistance in Egfr-Mutant Non-Small Cell Lung Cancer[J]. Clin Cancer Res. 2023, 29 (18): 3579–3591
4. S. Wang, Y. Song, F. Yan, D. Liu. Mechanisms of Resistance to Third-Generation Egfr Tyrosine Kinase Inhibitors[J]. Front Med. 2016, 10 (4): 383–388
5. E. Arnaiz, C. Sole, L. Manterola, L. Iparraguirre, D. Otaegui, C.H. Lawrie. Circrnas and Cancer: Biomarkers and Master Regulators[J]. Semin Cancer Biol. 2019, 58: 90–99
6. J. Li, D. Sun, W. Pu, J. Wang, Y. Peng. Circular Rnas in Cancer: Biogenesis, Function, and Clinical Significance[J]. Trends Cancer. 2020, 6 (4): 319–336
7. C. Wang, C. Ju, D. Du, P. Zhu, J. Yin, J. Jia, et al. Circnf1 Modulates the Progression and Immune Evasion of Esophageal Squamous Cell Carcinoma through Dual Regulation of Pd-L1[J]. Cell Mol Biol Lett. 2025, 30 (1): 37
8. P.F. Zhang, X. Pei, K.S. Li, L.N. Jin, F. Wang, J. Wu, et al.Circular Rna Circfgfr1 Promotes Progression and Anti-Pd-1 Resistance by Sponging Mir-381-3p in Non-Small Cell Lung Cancer Cells[J]. Mol Cancer. 2019, 18 (1): 179
9. J. Li, X. Xu, K. Xu, X. Zhou, K. Wu, Y. Yao, et al. N6-Methyladenosine-Modified Circslco1b3 Promotes Intrahepatic Cholangiocarcinoma Progression Via Regulating Hoxc8 and Pd-L1[J]. J Exp Clin Cancer Res. 2024, 43 (1): 119

10. H. Hu, J. Tang, H. Wang, X. Guo, C. Tu, Z. Li. The Crosstalk between Alternative Splicing and Circular Rna in Cancer: Pathogenic Insights and Therapeutic Implications[J]. Cell Mol Biol Lett. 2024, 29 (1): 142
11. S. Schreiner, A. Didio, L.H. Hung, A. Bindereif. Design and Application of Circular Rnas with Protein-Sponge Function[J]. Nucleic Acids Res. 2020, 48 (21): 12326–12335
12. X. Zhang, S. Yang, Z. Kang, W. Ru, X. Shen, M. Li, et al. Circmef2d Negatively Regulated by Hnrnpa1 Inhibits Proliferation and Differentiation of Myoblasts Via Mir-486-Pi3k/Akt Axis[J]. J Agric Food Chem. 2022, 70 (26): 8145–8163
13. P. Montañés-Agudo, I. van der Made, S. Aufiero, A.J. Tijsen, Y.M. Pinto, E.E. Creemers. Quaking Regulates Circular Rna Production in Cardiomyocytes[J]. J Cell Sci. 2023, 136 (13)
14. L.D. Hou, J. Zhang. Circular Rnas: An Emerging Type of Rna in Cancer[J]. Int J Immunopathol Pharmacol. 2017, 30 (1): 1–6
15. W. Zhao, M. Dong, J. Pan, Y. Wang, J. Zhou, J. Ma, et al. Circular Rnas: A Novel Target among Non–Coding Rnas with Potential Roles in Malignant Tumors (Review)[J]. Mol Med Rep. 2019, 20 (4): 3463–3474
16. W.W. Du, L. Fang, W. Yang, N. Wu, F.M. Awan, Z. Yang, et al. Induction of Tumor Apoptosis through a Circular Rna Enhancing Foxo3 Activity[J]. Cell Death Differ. 2017, 24 (2): 357–370
17. X. Zang, J. Jiang, J. Gu, Y. Chen, M. Wang, Y. Zhang, et al. Circular Rna Eif4g3 Suppresses Gastric Cancer Progression through Inhibition of B-Catenin by Promoting Δ-Catenin Ubiquitin Degradation and Upregulating Sik1[J]. Mol Cancer. 2022, 21 (1): 141
18. X. Chen, R. Mao, W. Su, X. Yang, Q. Geng, C. Guo, et al.Circular Rna Circhipk3 Modulates Autophagy Via Mir124-3p-Stat3-Prkaa/Ampkα Signaling in Stk11 Mutant Lung Cancer[J]. Autophagy. 2020, 16 (4): 659–671
19. G. Liang, Y. Ling, M. Mehrpour, P.E. Saw, Z. Liu, W. Tan, et al.Autophagy-Associated Circrna Circcdyl Augments Autophagy and Promotes Breast Cancer Progression[J]. Mol Cancer. 2020, 19 (1): 65
20. S.J. Conn, K.A. Pillman, J. Toubia, V.M. Conn, M. Salmanidis, C.A. Phillips, et al.The Rna Binding Protein Quaking Regulates Formation of Circrnas[J]. Cell. 2015, 160 (6): 1125–1134
21. P. Han, P. Cao, J. Yue, K. Kong, S. Hu, Y. Deng, et al.Knockdown of Hnrnpa1 Promotes Nsclc Metastasis and Emt by Regulating Alternative Splicing of Las1l Exon 9[J]. Front Oncol. 2022, 12: 837248
22. J.C. Soria, Y. Ohe, J. Vansteenkiste, T. Reungwetwattana, B. Chewaskulyong, K.H. Lee, et al.Osimertinib in Untreated Egfr-Mutated Advanced Non-Small-Cell Lung Cancer[J]. N Engl J Med. 2018, 378 (2): 113–125
23. S.S. Ramalingam, J. Vansteenkiste, D. Planchard, B.C. Cho, J.E. Gray, Y. Ohe, et al.Overall Survival with Osimertinib in Untreated, Egfr-Mutated Advanced Nsclc[J]. N Engl J Med. 2020, 382 (1): 41–50
24. Z. Piotrowska, H. Isozaki, J.K. Lennerz, J.F. Gainor, I.T. Lennes, V.W. Zhu, et al.Landscape of Acquired Resistance to Osimertinib in Egfr-Mutant Nsclc and Clinical Validation of Combined Egfr and Ret

Inhibition with Osimertinib and Blu-667 for Acquired Ret Fusion[J]. Cancer Discov. 2018, 8 (12): 1529–1539

25. A.J. Schoenfeld, J.M. Chan, D. Kubota, H. Sato, H. Rizvi, Y. Daneshbod, et al. Tumor Analyses Reveal Squamous Transformation and Off-Target Alterations as Early Resistance Mechanisms to First-Line Osimertinib in Egfr-Mutant Lung Cancer[J]. Clin Cancer Res. 2020, 26 (11): 2654–2663
26. G. Gomatou, N. Syrigos, E. Kotteas. Osimertinib Resistance: Molecular Mechanisms and Emerging Treatment Options[J]. Cancers (Basel). 2023, 15 (3)
27. L.S. Kristensen, M.S. Andersen, L.V.W. Stagsted, K.K. Ebbesen, T.B. Hansen, J. Kjems. The Biogenesis, Biology and Characterization of Circular Rnas[J]. Nat Rev Genet. 2019, 20 (11): 675–691
28. L.L. Chen. The Expanding Regulatory Mechanisms and Cellular Functions of Circular Rnas[J]. Nat Rev Mol Cell Biol. 2020, 21 (8): 475–490
29. T.B. Hansen, T.I. Jensen, B.H. Clausen, J.B. Bramsen, B. Finsen, C.K. Damgaard, et al. Natural Rna Circles Function as Efficient Microrna Sponges[J]. Nature. 2013, 495 (7441): 384–388
30. M. Daugaard, M. Rohde, M. Jäättelä. The Heat Shock Protein 70 Family: Highly Homologous Proteins with Overlapping and Distinct Functions[J]. FEBS Lett. 2007, 581 (19): 3702–3710
31. M.V. Powers, P. Workman. Inhibitors of the Heat Shock Response: Biology and Pharmacology[J]. FEBS Lett. 2007, 581 (19): 3758–3769
32. Y. Yuan, X. Zhang, X. Fan, Y. Peng, Z. Jin. The Emerging Roles of Circular Rna-Mediated Autophagy in Tumorigenesis and Cancer Progression[J]. Cell Death Discov. 2022, 8 (1): 385
33. S.Y. Kim, S.M. Kim, S. Lim, J.Y. Lee, S.J. Choi, S.D. Yang, et al. Modeling Clinical Responses to Targeted Therapies by Patient-Derived Organoids of Advanced Lung Adenocarcinoma[J]. Clin Cancer Res. 2021, 27 (15): 4397–4409
34. H. Zhao, Q. Zhou, X. Li. Protein Bait Hypothesis: Circrna-Encoded Proteins Competitively Inhibit Cognate Functional Isoforms[J]. Trends Genet. 2021, 37 (7): 616–624
35. M.S. Hipp, P. Kasturi, F.U. Hartl. The Proteostasis Network and Its Decline in Ageing[J]. Nat Rev Mol Cell Biol. 2019, 20 (7): 421–435
36. I. Dikic, B.A. Schulman. An Expanded Lexicon for the Ubiquitin Code[J]. Nat Rev Mol Cell Biol. 2023, 24 (4): 273–287
37. M.J. Clague, S. Urbé, D. Komander. Breaking the Chains: Deubiquitylating Enzyme Specificity Begets Function[J]. Nat Rev Mol Cell Biol. 2019, 20 (6): 338–352
38. E.T. Powers, W.E. Balch. Diversity in the Origins of Proteostasis Networks–a Driver for Protein Function in Evolution[J]. Nat Rev Mol Cell Biol. 2013, 14 (4): 237–248
39. S.B. Qian, H. McDonough, F. Boellmann, D.M. Cyr, C. Patterson. Chip-Mediated Stress Recovery by Sequential Ubiquitination of Substrates and Hsp70[J]. Nature. 2006, 440 (7083): 551–555
40. M. Gamerdinger, A.M. Kaya, U. Wolfrum, A.M. Clement, C. Behl. Bag3 Mediates Chaperone-Based Aggresome-Targeting and Selective Autophagy of Misfolded Proteins[J]. EMBO Rep. 2011, 12 (2): 149–156

41. S. Takayama, T. Sato, S. Krajewski, K. Kochel, S. Irie, J.A. Millan, et al.Cloning and Functional Analysis of Bag-1: A Novel Bcl-2-Binding Protein with Anti-Cell Death Activity[J]. Cell. 1995, 80 (2): 279–284
42. K.K. Deol, S.O. Crowe, J. Du, H.A. Bisbee, R.G. Guenette, E.R. Strieter. Proteasome-Bound Uch37/Uchl5 Debranches Ubiquitin Chains to Promote Degradation[J]. Mol Cell. 2020, 80 (5): 796–809.e799
43. C. Liu, W. Lou, J.C. Yang, L. Liu, C.M. Armstrong, A.P. Lombard, et al. Proteostasis by Stub1/Hsp70 Complex Controls Sensitivity to Androgen Receptor Targeted Therapy in Advanced Prostate Cancer[J]. Nat Commun. 2018, 9 (1): 4700
44. L. Li, Y. Wang, L. Jiao, C. Lin, C. Lu, K. Zhang, et al. Protective Autophagy Decreases Osimertinib Cytotoxicity through Regulation of Stem Cell-Like Properties in Lung Cancer[J]. Cancer Lett. 2019, 452: 191–202
45. G. Mariño, M. Niso-Santano, E.H. Baehrecke, G. Kroemer. Self-Consumption: The Interplay of Autophagy and Apoptosis[J]. Nat Rev Mol Cell Biol. 2014, 15 (2): 81–94
46. X. Sui, R. Chen, Z. Wang, Z. Huang, N. Kong, M. Zhang, et al.Autophagy and Chemotherapy Resistance: A Promising Therapeutic Target for Cancer Treatment[J]. Cell Death Dis. 2013, 4 (10): e838
47. A. Thorburn. Apoptosis and Autophagy: Regulatory Connections between Two Supposedly Different Processes[J]. Apoptosis. 2008, 13 (1): 1–9
48. B. Levine, G. Kroemer. Biological Functions of Autophagy Genes: A Disease Perspective[J]. Cell. 2019, 176 (1–2): 11–42
49. S. Huang, K. Okamoto, C. Yu, F.A. Sinicrope. P62/Sequestosome-1 up-Regulation Promotes Abt-263-Induced Caspase-8 Aggregation/Activation on the Autophagosome[J]. J Biol Chem. 2013, 288 (47): 33654–33666
50. Z. Qiu, Y. Wang, W. Liu, C. Li, R. Zhao, X. Long, et al. Circhipk3 Regulates the Autophagy and Apoptosis of Hypoxia/Reoxygenation-Stimulated Cardiomyocytes Via the Mir-20b-5p/Atg7 Axis[J]. Cell Death Discov. 2021, 7 (1): 64
51. Y. Wei, S. Pattingre, S. Sinha, M. Bassik, B. Levine. Jnk1-Mediated Phosphorylation of Bcl-2 Regulates Starvation-Induced Autophagy[J]. Mol Cell. 2008, 30 (6): 678–688
52. M.B. Løvendorf, A. Holm, A. Petri, C.A. Thrue, S. Uchida, M.T. Venø, et al. Knockdown of Circular Rnas Using Lna-Modified Antisense Oligonucleotides[J]. Nucleic Acid Ther. 2023, 33 (1): 45–57
53. M. Kordyś, R. Sen, Z. Warkocki. Applications of the Versatile Crispr-Cas13 Rna Targeting System[J]. Wiley Interdiscip Rev RNA. 2022, 13 (3): e1694
54. F. Zhang, J. Jiang, H. Qian, Y. Yan, W. Xu. Exosomal Circrna: Emerging Insights into Cancer Progression and Clinical Application Potential[J]. J Hematol Oncol. 2023, 16 (1): 67
55. X. Wu, M. Shi, Y. Lian, H. Zhang. Exosomal Circrnas as Promising Liquid Biopsy Biomarkers for Glioma[J]. Front Immunol. 2023, 14: 1039084

Figures

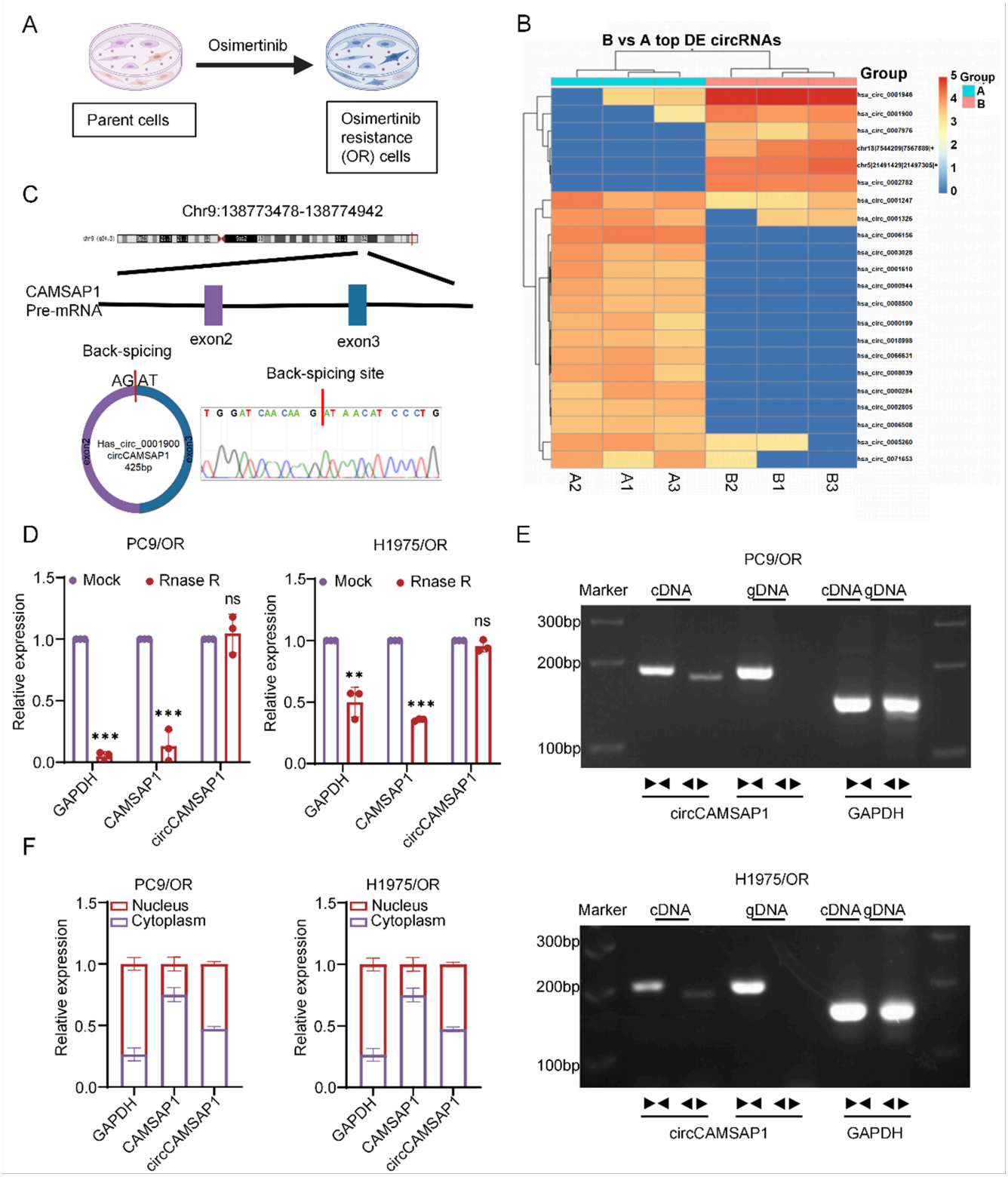


Figure 1

CircCAMSAP1 is identified as a highly upregulated circular RNA in osimertinib-resistant NSCLC cells. A Schematic diagram of the construction of osimertinib-resistant PC9/OR and H1975/OR cells for lung adenocarcinoma. B Cluster heat map of 8 significantly upregulated and 14 downregulated circRNAs in parental cells (PC9) and drug-resistant cells (PC9/OR) by high-throughput sequencing analysis of circRNAs, with an expression level of >2.0 and a p-value of <0.05, indicating a statistically significant

difference.C Schematic diagram of the genomic location and splicing pattern of CircCAMSAP1, with Sanger sequencing confirming the splice junction site.D Semi-quantitative RT-PCR was used to verify the expression of divergent primers (circCAMSAP1) and convergent primers (CAMSAP1) in cDNA and gDNA, with GAPDH as an internal control.E Expression of circCAMSAP1 and CAMSAP1 in PC9/OR and H1975/OR cell lines was detected by RT-qPCR with or without RNAse R digestion.F Cytoplasmic-nuclear separation assay to detect the subcellular localization of circCAMSAP1 in PC9/OR and H1975/OR cells. GAPDH as a cytoplasmic internal control and U1 as a nuclear internal control. ** P<0.01,*** P<0.001,ns difference was not significant

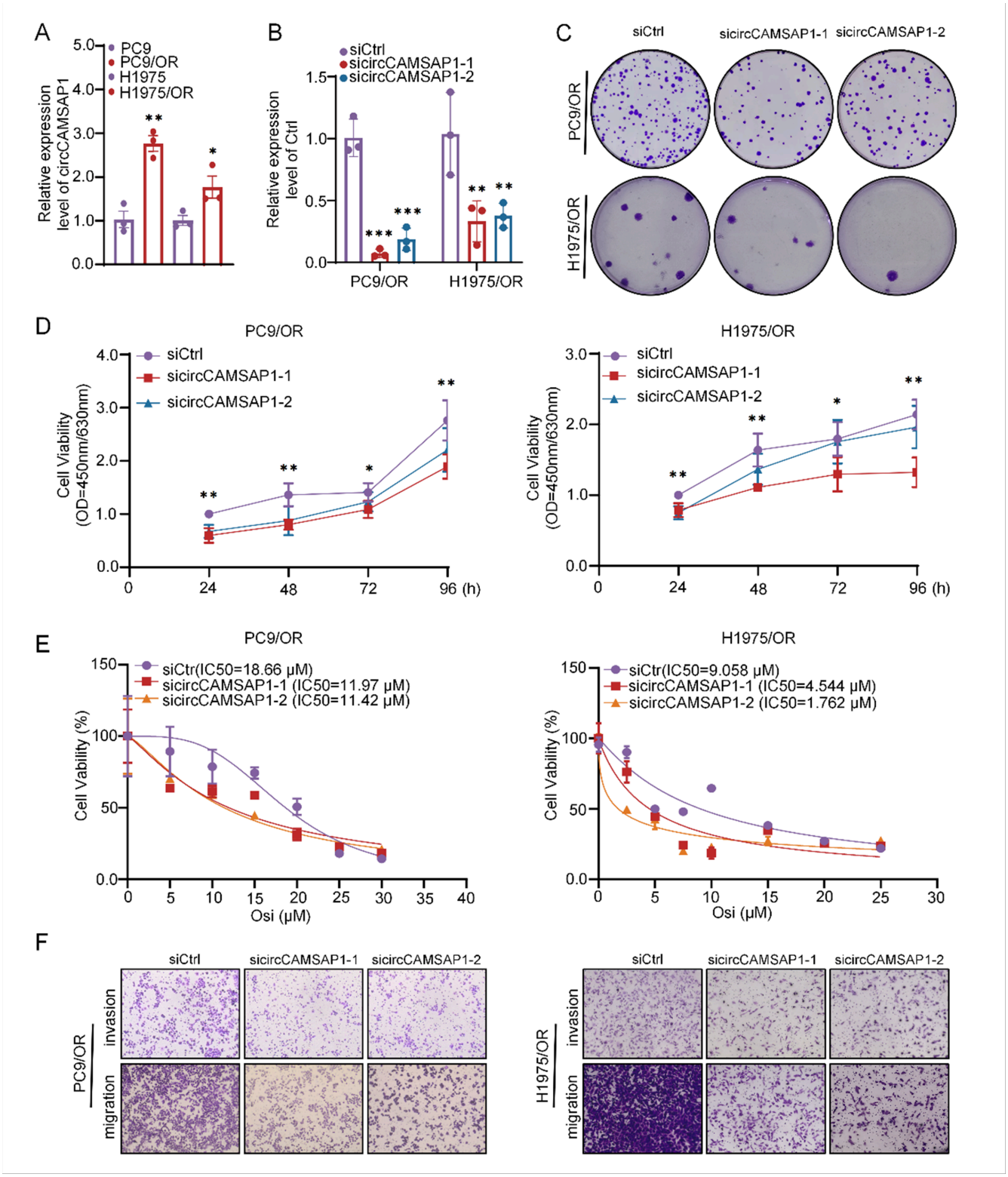


Figure 2

CircCAMSAP1 promotes proliferation, migration, invasion, and osimertinib resistance in NSCLC cells. A RT-qPCR analysis was used to detect the expression of circCAMSAP1 in osimertinib-sensitive cell lines (PC9 and H1975) and drug-resistant cell lines (PC9/OR and H1975/OR). B RT-qPCR analysis of the knockout efficiency of circCAMSAP1 transfected with sicircCAMSAP1 in PC9/OR and H1975/OR cells; C To evaluate the clonal formation capacity of PC9/OR and H1975/OR cells after knockdown of

circCAMSAP1 by colony formation assay; D Proliferation ability of PC9/OR and H1975/OR cells after circCAMSAP1 knockdown was detected by WST-1 assay. E Knockdown of circCAMSAP1 in different doses of osimertinib treatment to assess PC9/OR and H1975/OR cell viability; F To evaluate the invasion and migration capacity of PC9/OR and H1975/OR cells after knockdown of circCAMSAP1 by transwell assay. * P<0.05 ** P<0.01 *** P<0.001

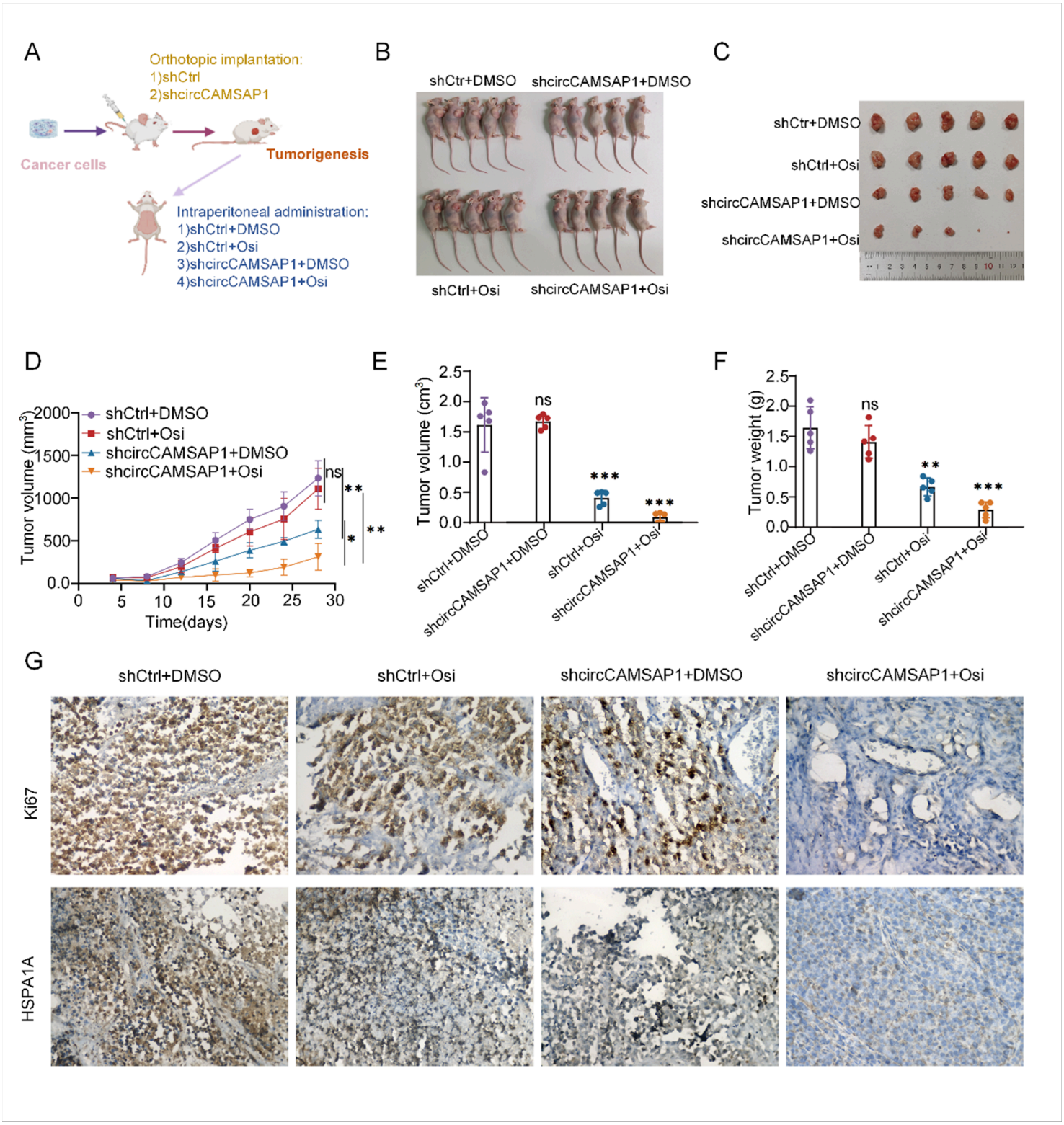


Figure 3

CircCAMSAP1 facilitates tumor growth and resistance to osimertinib in vivo. A Schematic diagram of subcutaneous tumor formation in BALB/c nude mice (4- to 6-week-old females) with knockdown of circCAMSAP1 in PC9/OR cells. B-C BALB/c nude mice were subcutaneously inoculated with shCtrl and shcircCAMSAP1 cells of PC9/OR, treated with DMSO or osimertinib (5mg/kg/alternate day), and mice were euthanized by cervical dislocation method, and the mouse was euthetically infused with subcutaneous tumor images (n=5). D Tumor volume was measured and xenograft tumor growth curves were plotted. E Tumor volume measured after 28 days of treatment (n=5). F Tumor weight measured after 28 days of treatment (n=5). g Immunohistochemistry to detect the expression of Ki-67 and HSPA1A in xenograft tumors in different treatment groups. * $P<0.05$, ** $P<0.01$, *** $P<0.001$, ns difference is not significant

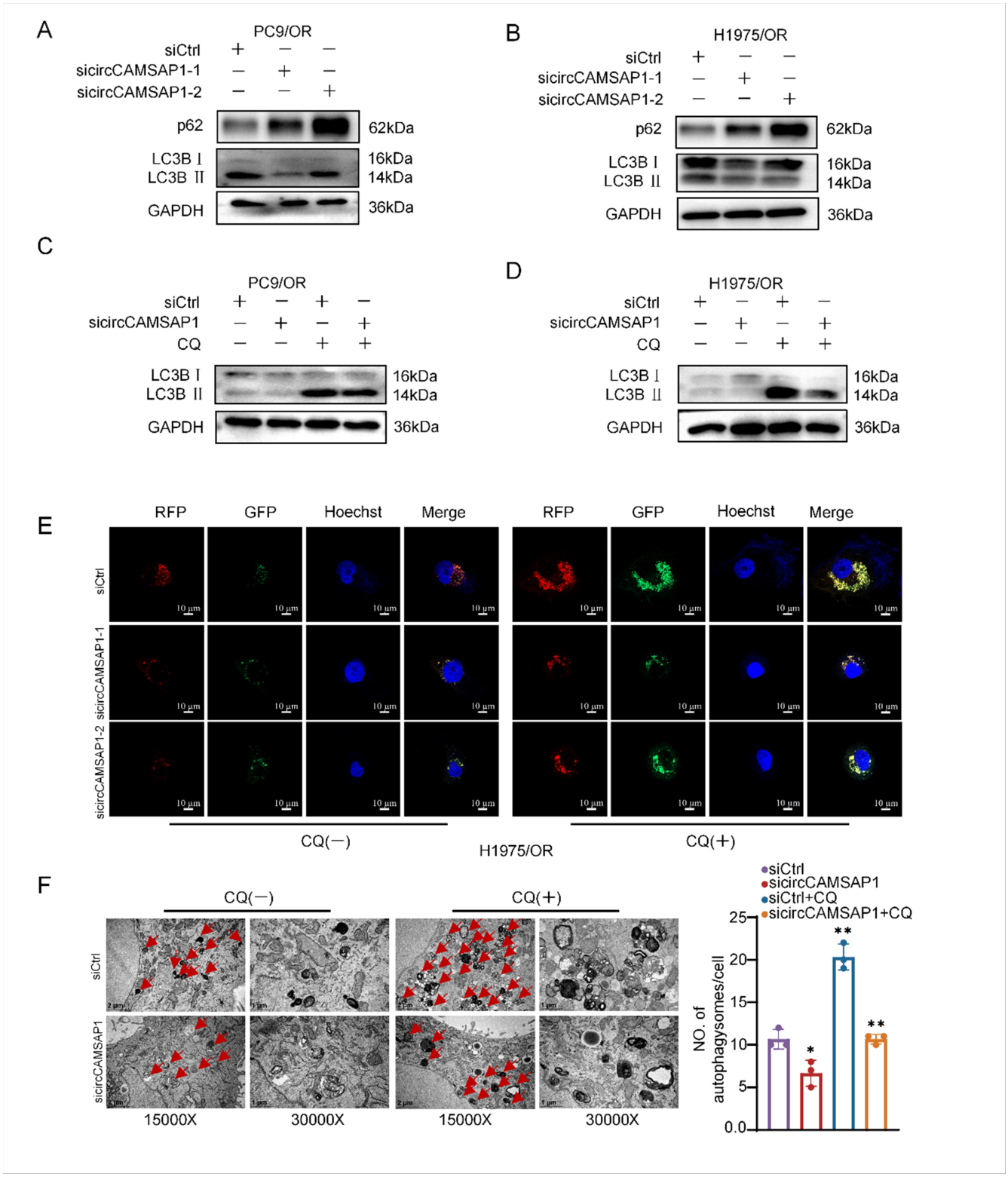


Figure 4

CircCAMSAP1 facilitates autophagic activity in resistant NSCLC cells. A-B The expression of autophagy-related proteins in PC9/OR and H1975/OR cells after knockdown of circCAMSAP1 was detected by Western blotting. C-D Autophagy-associated protein expression in PC9/OR and H1975/OR cells with or without CQ treatment after knockdown of circCAMSAP1 was detected by Western blotting. E Representative image of autophagosomes of H1975/OR cells transfected with RFP-GFP-LC3 lentivirus

after knockdown of circCAMSAP1 detected by confocal microscopy with or without CQ treatment. F Autophagosomes of H1975/OR cells that knock down circCAMSAP1 were examined with transmission electron microscopy (TEM), with or without CQ treatment in the cells, and the autophagosomes are indicated by red arrows. * P□0.05□** P□0.01

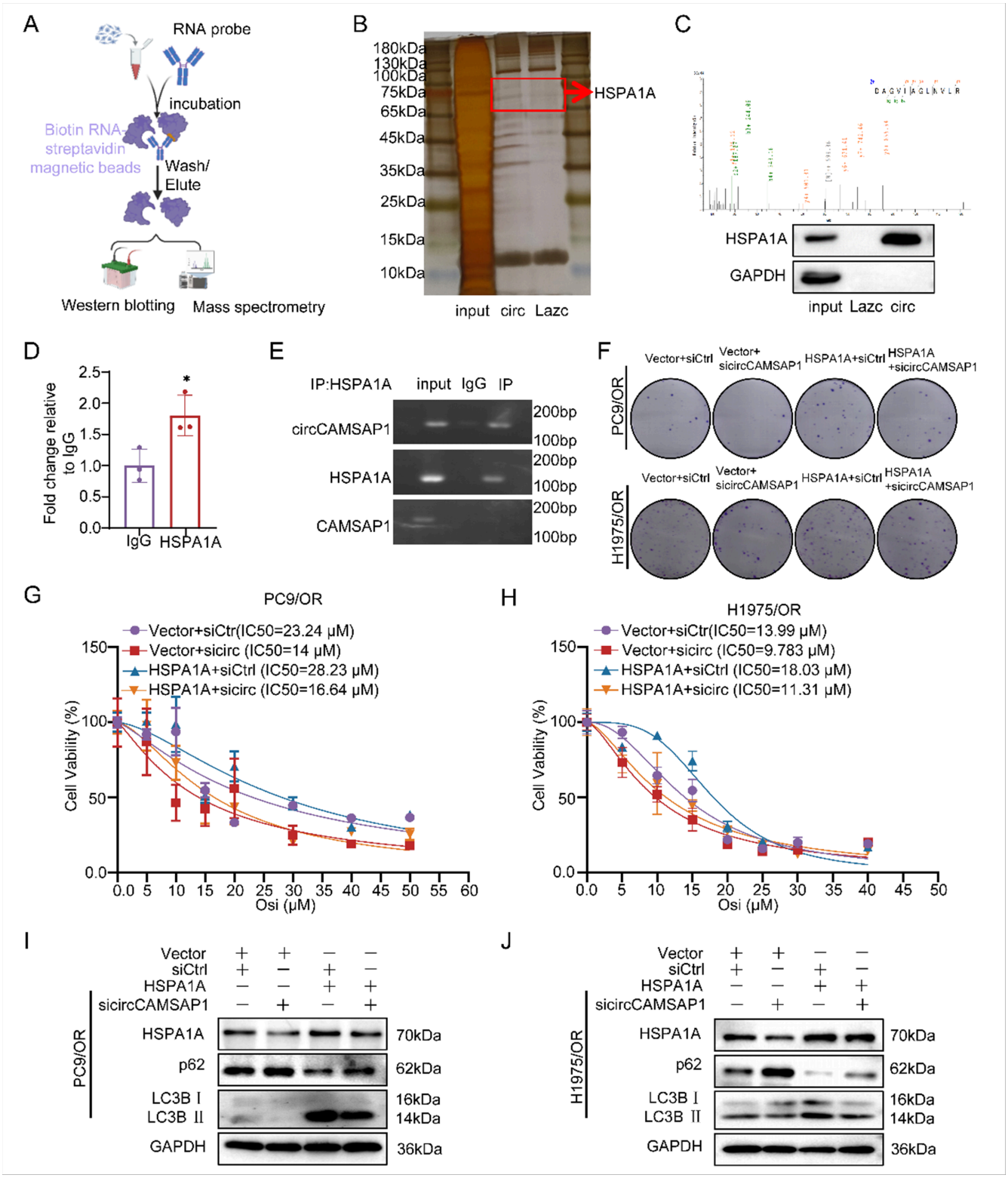


Figure 5

CircCAMSAP1 binds to HSPA1A and enhances its expression to sustain resistance and autophagy. A Schematic diagram of RNA pulldown and mass spectrometry to detect the potential effects of circCAMSAP1 on circCAMSAP1; B Silver-stained image of the SDS-PAGE gel, showing the isolation of circCAMSAP1/protein complexes from RNA pulldown experiments in PC9/OR cells, with red boxes highlighting specific protein bands enriched by circCAMSAP1 probes in RNA pulldown complexes compared to Lazc probes; C Identification of HSPA1A protein-specific peptides by mass spectrometry and Western blotting after RPD to confirm the interaction between circCAMSAP1 and HSPA1A; D-E RIP and semi-quantitative RT-qPCR assays showed verification of interactions between HSPA1A and circCAMSAP1 using anti-HSPA1A antibodies; F To assess the clonal forming capacity of PC9/OR and H1975/OR cells after knockdown of circCAMSAP1 and/or overexpression of HSPA1A by colony formation assays; G-H assessed PC9/OR and H1975/OR cell viability by knocking down circCAMSAP1 and/or overexpressing HSPA1A in different doses of osimertinib treatment; I-J Detection of autophagy-related protein expression in PC9/OR and H1975/OR cells after knockdown of circCAMSAP1 and/or overexpression of HSPA1A by Western blotting. * P□0.01

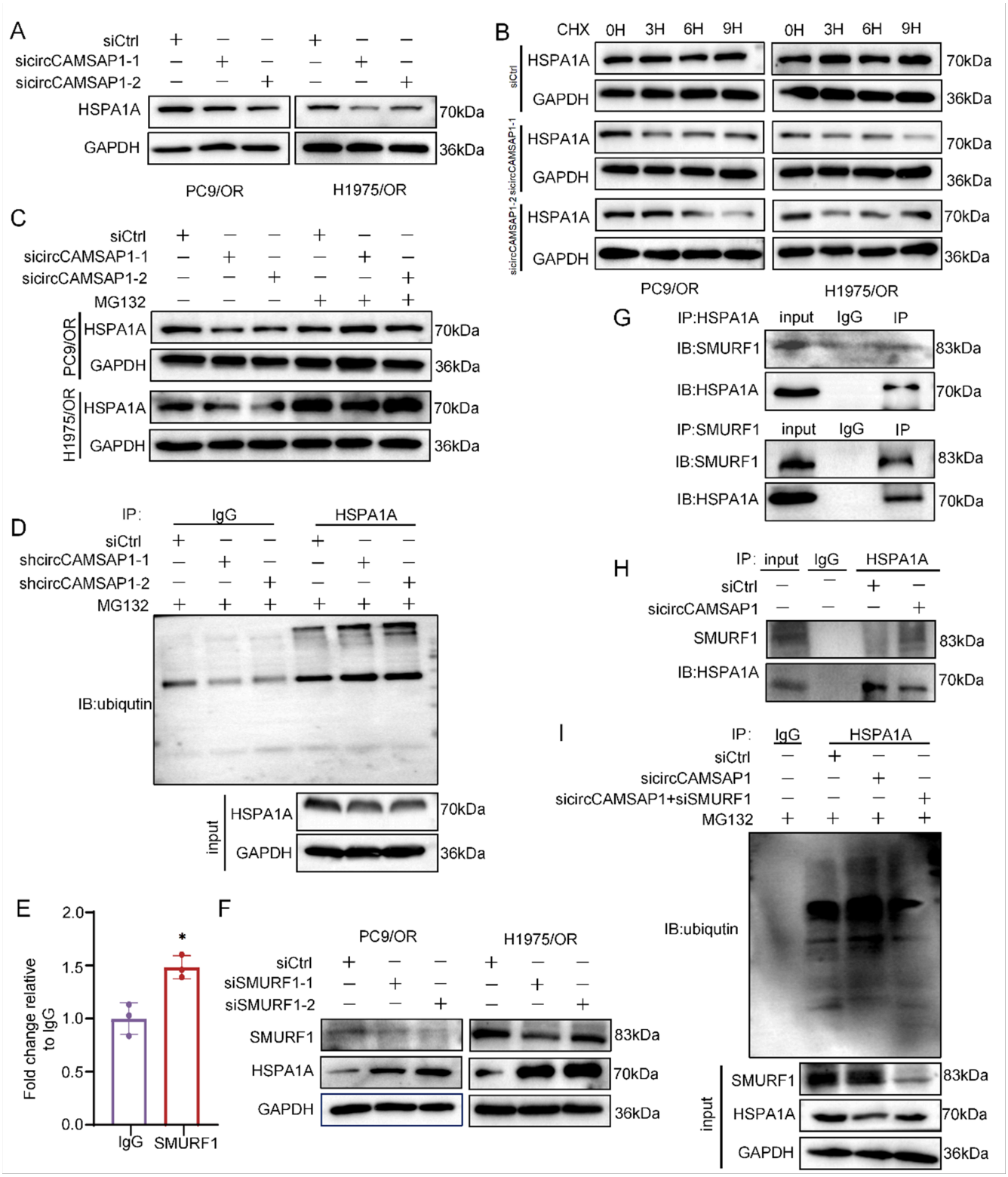


Figure 6

CircCAMSAP1 stabilizes HSPA1A protein by blocking SMURF1-mediated ubiquitination. A Western blotting to detect the effect of knockdown of circCAMSAP1 on the expression level of HSPA1A protein. B HSPA1A protein stability was detected by western blot by Western blot after knockdown of circCAMSAP1 and treated with actinomycone (CHX) at different time points. C After knocking down circCAMSAP1, the proteasome inhibitor MG132 (10 μM) was used for 6 hours, and the HSPA1A protein

level was detected by Western blotting. D After knockdown of circCAMSAP1, PC9/OR cells were treated with MG-132 (10 μM) to detect the level of ubiquitination modification of HSPA1A protein by immunoprecipitation (Co-IP) assay. E RIP and RT-qPCR assays showed that the interaction between SMURF1 and circCAMSAP1 was verified using anti-SMURF1 antibodies. F Detection of the effect of knockdown of SMURF1 on the expression levels of SMURF1 and HSPA1A proteins by Western blotting. G Co-immunoprecipitation (Co-IP) assay to detect the interaction between SMURF1 and HSPA1A. H Co-immunoprecipitation (Co-IP) assay detected that knockdown of circCAMSAP1 promotes the interaction between SMURF1 and HSPA1A. I After co-transfection of sicircCAMSAP1 and siSMURF1, the level of ubiquitination modification of HSPA1A protein was detected by immunoprecipitation (Co-IP) assay after treatment of PC9/OR cells with MG-132 (10 μM). * P□0.05

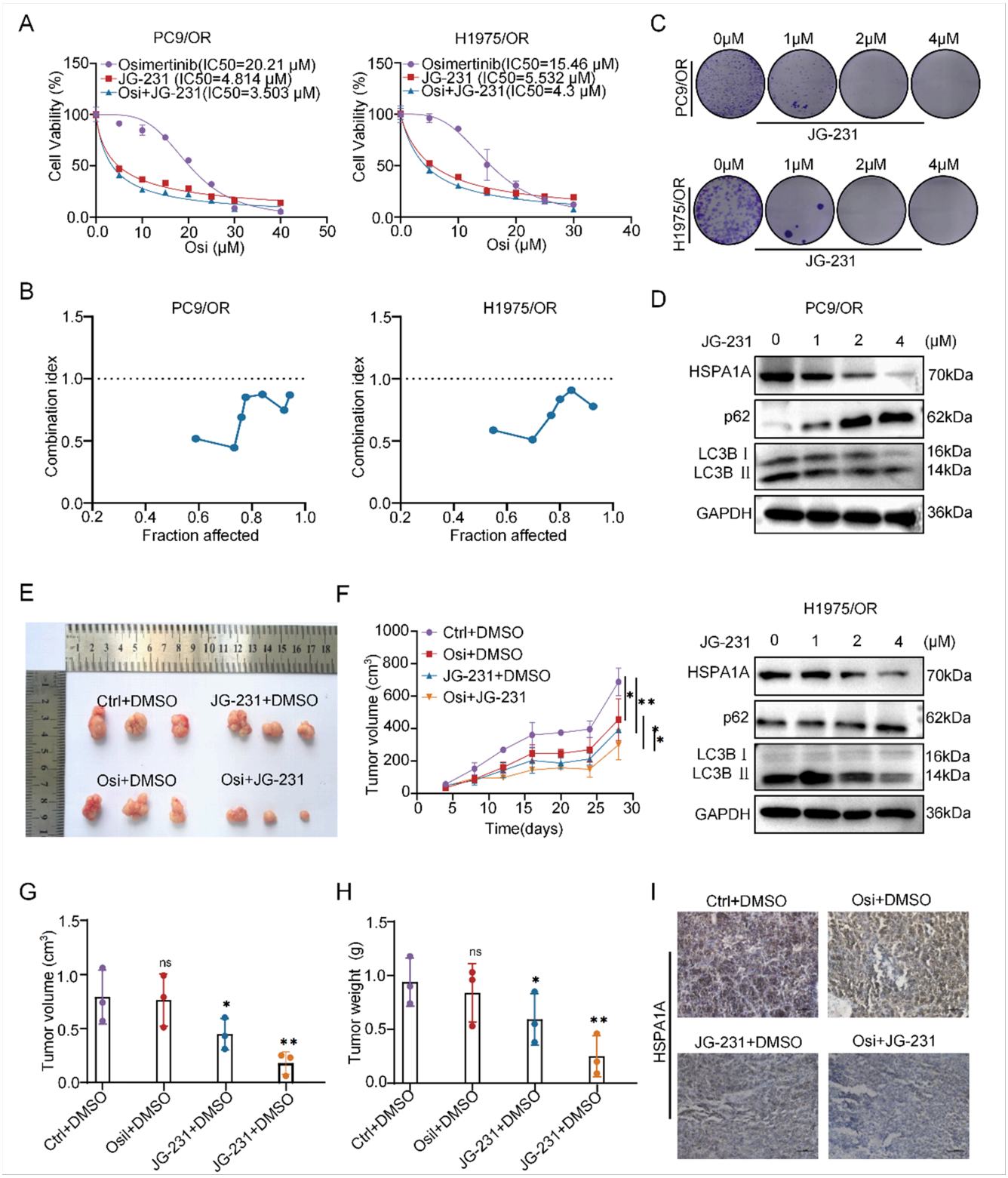


Figure 7

The allosteric inhibitor JG231 reverses osimertinib resistance in lung adenocarcinoma in vitro and in vivo. A Evaluate PC9/OR and H1975/OR cell viability by WST-1 method in different doses of JG231 and osimertinib treatment. B Combined index (CI) of osimertinib and JG231 combination therapy for 24 hours. C Treatment of PC9/OR and H1975/OR cells with escalating concentrations of JG231 (0, 1, 2, 4 μM) for 24 h, and the clonal formation capacity of cells was evaluated by colony formation assay. D

Protein levels and autophagy-related protein expression of HSPA1A were detected by Western blot in PC9/OR and H1975/OR cells treated with JG231 (0, 1, 2, 4μM) at increasing concentrations for 24 h. E BALB/c nude mice were subcutaneously inoculated with PC9/OR cells with DMSO, osimertinib (5mg/kg/next day), JG231 (4mg/kg/i.P.) After treatment, mice were euthanized by cervical dislocation method, and the subcutaneous tumor image of the mice (n=3). F Tumor volume was measured and the growth curve of xenograft tumors was drawn. G Tumor volume was measured after 28 days of treatment (n=3). H. Tumor weight measured after 28 days of treatment (n=3). I Immunohistochemistry to detect the expression of HSPA1A in xenograft tumors in different treatment groups. * $P<0.05$, ** $P<0.01$, ns ns There was no significant difference

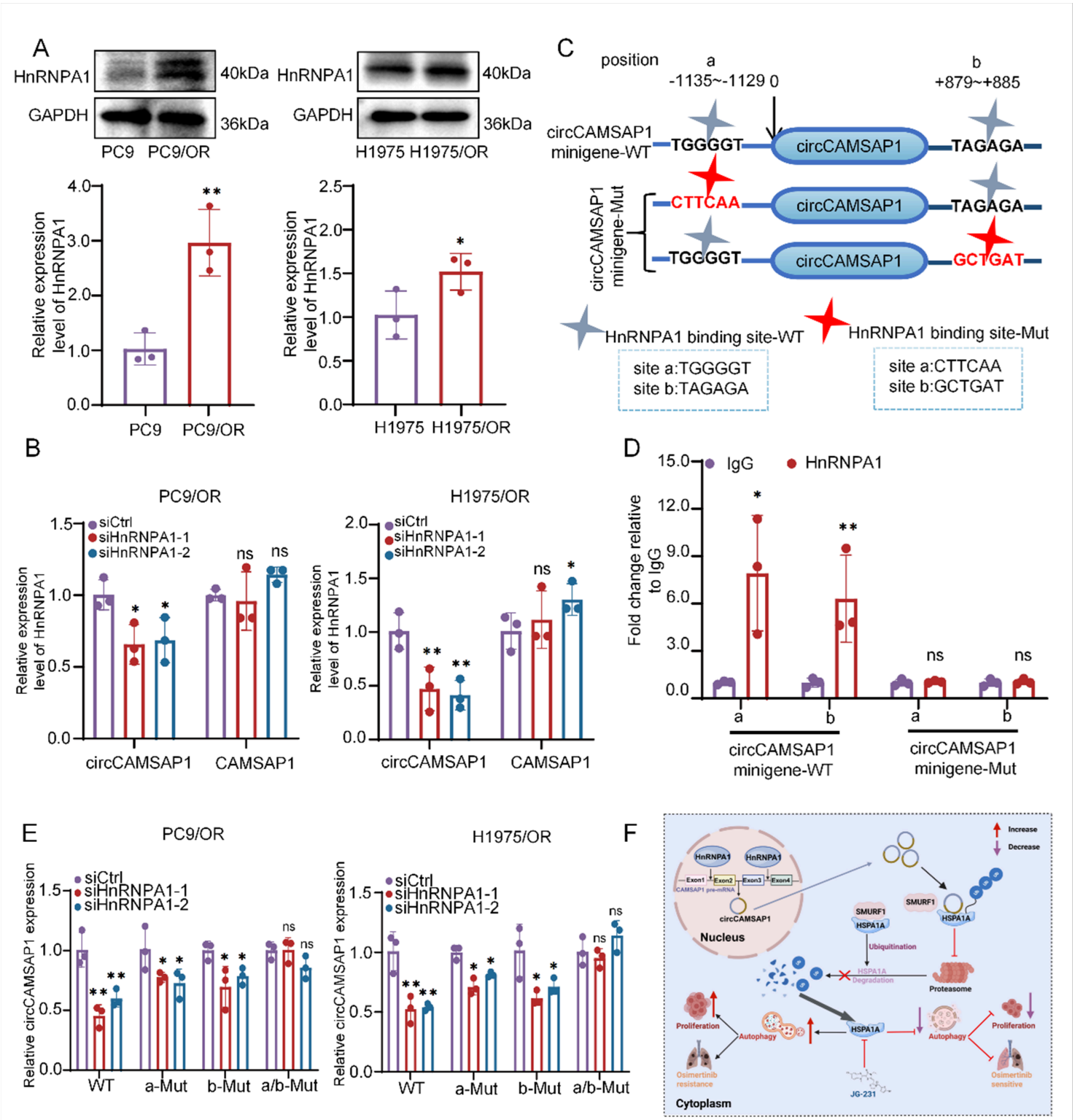


Figure 8

HnRNPA1 promotes the biogenesis of circCAMSAP1. A Western blot and RT-qPCR analysis were used to detect the expression of HnRNPA1 in osimertinib-sensitive cell lines (PC9 and H1975) and drug-resistant cell lines (PC9/OR and H1975/OR). B Effect of knockdown of HnRNPA1 on circCAMSAP1 and linear CAMSAP1 mRNA levels detected by RT-qPCR analysis. C Schematic diagram of the circCAMSAP1 minigene with two wild-type (WT) or mutant (Mut) HnRNPA1 binding sites. D RIP analysis of HnRNPA1-

binding wild-type (WT) or mutant (Mut) circCAMSAP1 minigenes using anti-HnRNPA1 antibodies. E RT-qPCR analysis of circCAMSAP1 after co-transfection with siHnRNPA1 or siCtrl and wild-type (WT) or various mutant (Mut) circCAMSAP1 minigenes. F Schematic diagram of the HnRNPA1/circCAMSAP1/SMURF1/HSPA1A signaling pathway inducing autophagy to promote osimertinib resistance in lung adenocarcinoma. * P<0.05, ** P<0.01, ns difference was not significant

Supplementary Files

This is a list of supplementary files associated with this preprint. Click to download.

- Primer.docx
- siRNA.docx
- SupplementaryMaterials.docx